UNIVERSITAT POLITÈCNICA DE VALÈNCIA

Escuela Técnica Superior de Ingeniería del Diseño

UNIVERSITAT POLITÈCNICA DE VALÈNCIA

Escuela Técnica Superior de Ingeniería del Diseño

Control y efecto de las perturbaciones con el uso de correas electromagnéticas en órbitas LEO

Trabajo Fin de Grado

Grado en Ingeniería Aeroespacial

AUTOR/A: Pérez Castañosa, Jorge

Tutor/a: Moll López, Santiago Emmanuel

Cotutor/a externo: VEGA FLEITAS, ERICA

CURSO ACADÉMICO: 2021/2022

UNIVERSITAT POLITÈCNICA DE VALÈNCIA

Bachelor's degree thesis

Control and effect of the perturbations using electrodynamic tethers in LEO orbits

Author

Jorge Pérez Castañosa

Supervisors

Santiago Emmanuel Moll López

Erika Vega Fleitas

Bachelor's Degree in Aerospace Engineering

Academic Year 2021 - 2022

Escuela Técnica Superior de Ingeniería del Diseño

Universitat Politècnica de València

Valencia - July 2022

Dedicated to my family
and to my friends of UTK
especially to Javier
for this 4 years.

Abstract

The objective of this project is the study of Low Earth Orbit (LEO) satellites under the influence of electrodynamic tethers (EDTs) as a propulsive system. For this purpose, two-body equations will be implemented with the addition of the perturbations due to the geomagnetic field and the ionosphere interaction of the EDTs system. Likewise, the de-orbiting capabilities of the EDTs will be assessed by integrating an atmospheric model and the drag force. In addition, different initial conditions will be taken, and the effectiveness and the time needed to perform the required maneuvers in each situation will be tested.

Keywords: electrodynamic thethers, low earth orbits, magnetic field:

Resumen

El objetivo de este proyecto es el estudio de satélites en órbita terrestre baja (LEO) bajo la influencia de correas electromagnéticas (EDTs) como dispositivo de propulsión. Para ello se utilizarán las ecuaciones del movimiento relativo de dos cuerpos a las que se añadirá como perturbación la interacción con el campo magnético y la ionosfera del sistema de EDTs. Así mismo, se estudiarán las aplicaciones de estos sistemas propulsivos en la desorbitación de satélites integrando el modelo atmosférico y la fuerza de arrastre en el problema. Además, se tomarán distintas condiciones iniciales y se comprobará la efectividad y el tiempo necesario para efectuar las maniobras requeridas en cada situación.

Palabras clave: correas electromagnéticas, órbitas terrestres bajas, campo magnético

Contents

Nomenclature

Greek letters

α	Grid sphere transparency
Ω	Longitude of the ascending node
ω	Argument of the perigee
ϕ_{ind}	Induced Electromotive force
ρ	Air density
ρ_{lin}	Linear resistivity of the cable
θ	True anomaly

Latin letters

$\hat{F_B}$	Lorentz Force direction
$\hat{v}$	Velocity direction
$\vec{B}$	Magnetic field vector
$\vec{C}$	Laplace-Runge-Lenz vector
$\vec{e}$	Eccentricity
$\vec{F_B}$	Lorentz Force
$\vec{F_D}$	Drag Force
$\vec{r}$	Orbital radius modulus
$\vec{v_a}$	Aerodynamic velocity
$\vec{v}$	Orbital velocity
a	Semimajor axis
C_D	Drag coefficient of the satellite
h	Angular momentum
h	Height above Earth surface
I	Current along the tether
i	Orbit inclination
L_0	Reference length of the tether

m_s	Satellite mass	
n_∞	Plasma density	
r	Orbital radius modulus	
r_0	Iniital orbital radius	
S_0	Tether cable section	
S_f	Reference surface of the satellite	
S_{sph}	Grid sphere contact surface	
T_e	Plasma temperature	
v	Orbital speed	

Constants

μ	Standard gravitational parameter of the Earth	$3.986004418 \times 10^{14}\,\mathrm{m^3\,kg^{-2}}$
$\vec{\omega_E}$	Earth's angular speed	
B_0	Earth's magnetic field strength	$3.12 \times 10^{-5}\,\mathrm{kg\,s^{-2}\,A^{-1}}$
G	Universal gravitational constant	$6.67430 \times 10^{-11}\,\mathrm{m^3\,kg^{-1}\,s^{-2}}$
k	Boltzmann constant	$1.380649 \times 10^{-23}\,\mathrm{J\,K^{-1}}$
M_e	Earth mass	$5.9736 \times 10^{24}\,\mathrm{kg}$
m_e	Electron mass	$9.11 \times 10^{-31}\,\mathrm{kg}$
q_e	Elemental charge	$1.602 \times 10^{-19}\,\mathrm{C}$
R_E	Earth radius	$6.3781 \times 10^{6}\,\mathrm{m}$

List of Figures

List of Tables

Part I
Project report

1 Introduction

Spacecraft propulsion is described as a method to change the velocity of spacecraft and satellites. According to the operation place, the two main branches found inside spacecraft propulsion are: "In-space propulsion" (vacuum operated systems) and "Launching propulsion" (vacuum and atmospheric systems). Currently, launching propulsion is limited to chemical reaction engines (whether reaction or rocket engines) as they are the only ones capable of overcoming the Earth's gravitational field, providing enough speed for spacecraft to get into orbit.

This academic project is focused on the possibility of having non-chemical propulsion and, in particular, a fuel-free alternative that uses the electromagnetic field and ionosphere of the Earth known as "Electrodynamic tether."

1.1 Objectives

In order to develop the present bachelor thesis, the following objectives are stated:

- To define the elements present in an electrodynamic tether system and its working principle. Finding the physical laws that rule the behaviour and the components characteristics.
- To develop an algebraic model of the Earth's magnetic field to be able to operate with it.
- To acquire an algebraic or numerical model of the ionosphere and find the relation with the magnetic force.
- To obtain an algebraic or numerical model of the atmosphere density to model the drag force.
- To integrate the Lorentz and Drag forces into the two body equations.
- To explore the possible applications and simulate the orbital behaviour on them using MATLAB.
- To analyse the limitations of the electrodynamic tethers in space missions.

2 Electrodynamic tether system description

By definition, electrodynamic tethers are conductive wires that use a magnetic field to induce a voltage across them. They are deployed from a satellite to act as a de-orbiting system, power generator, or propulsive system [7]. In this section, there will be described the physical principles behind the operation of EDTs.

2.1 Working principle

As mentioned in the introduction of this section, EDTs are based on the interaction between magnetic and electric fields. A voltage is induced in a conductor in motion of a magnetic field according to Faraday's Law (Equation 1). The induced electromotive force (ϕ_{ind}) is proportional to vector product of the velocity of the conductor ($\vec{v}$) and the magnetic field ($\vec{B}$) integrated along the length of the conductor (L).

$$\phi_{ind} = \int_0^L (\vec{v} \times \vec{B}) \cdot dL = L_0 \cdot (\vec{v} \times B) \tag{1}$$

If the current flow is allowed, according to the definition of Lorentz force ($\vec{F_B}$), a current ($\vec{I}$) circulating along a conductor within a magnetic field ($\vec{B}$) generates a force perpendicular to the direction of the current and the magnetic field. If the conductor is rigid and the magnetic field and current are constant along all the conductor, the expression without an integral can be used:

$$\vec{F_B} = \int_L (\vec{I} \cdot dL \times \vec{B}) = \vec{I} \cdot L_0 \times \vec{B} \tag{2}$$

Moreover, the tether is assumed to be aligned radially with the Earth, so $\vec{I}$ can be expressed as a function of the spatial coordinates times the magnitude of the current. The sign will now depend on the orientation of the anode (Figures 1 and 2).

$$\vec{I} \cdot L_0 \times \vec{B} = \pm I \cdot L_0 \cdot \left\{ \frac{x}{r}, \frac{y}{r}, \frac{z}{r} \right\} \times \vec{B} \tag{3}$$

2.2 Operation modes

According to the definition, EDTs can be used as de-orbit devices and propulsive systems. In the following examples, a satellite in a prograde motion visualized from a polar top view will be used to explain the different modes.

De-orbit/energy harvesting mode

The de-orbit/energy harvesting mode uses the induced electromotive force ϕ_{ind} to drive a current in the outgoing direction from the Earth (pointing to the anode, as shown in Figure 1). If the objective is to obtain energy, the current would be dissipated in a battery. Whereas if the final objective is to de-orbit the satellite, the energy would be dissipated

in a resistor or a similar device. In both cases, the electromotive force is obtained at the expense of the orbital speed.

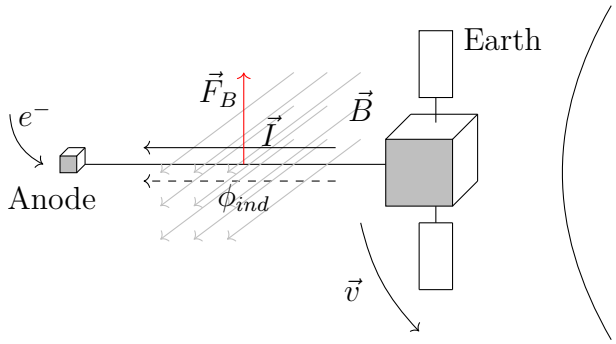

Figure 1: Schematic representation of the EDT in de-orbit/Energy harvesting mode (own elaboration)

Propulsive mode

The propulsive mode uses the Lorentz force to increase the orbital speed and, thus, to raise the satellite's orbit. As opposed to the de-orbit mode, the electromotive force induced cannot drive current in the direction imposed by the anode (Figure 2a). In order to produce a current in the allowed direction the ϕ_{ind} must be overcome by an external power supply (in this case, a High Voltage Power Supply). Then, the current would produce a Lorentz Force that boosts the satellite (Figure 2b).

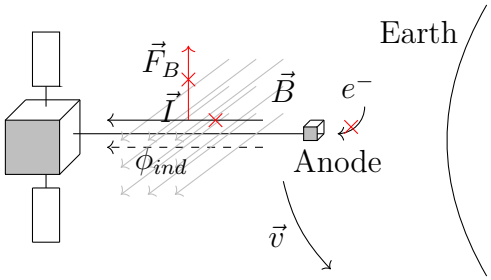

(a) Operation without an external source

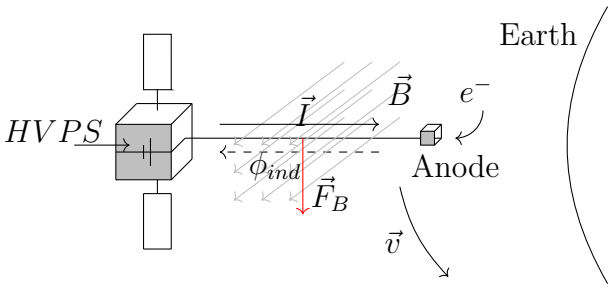

(b) Operation using a HVPS

Figure 2: Schematic representation of the EDT in boost mode (own elaboration)

2.2.1 Electric circuit

Taking into account the operation modes described in the previous section, it is possible to build an equivalent electric circuit for each of them.

The tether is modeled as a single resistor, while the cathode and anode are modeled as a resistor and a diode to implement the unidirectional current flow of the devices. In energy harvesting, the distinct element is the power generator between the tether and the cathode.

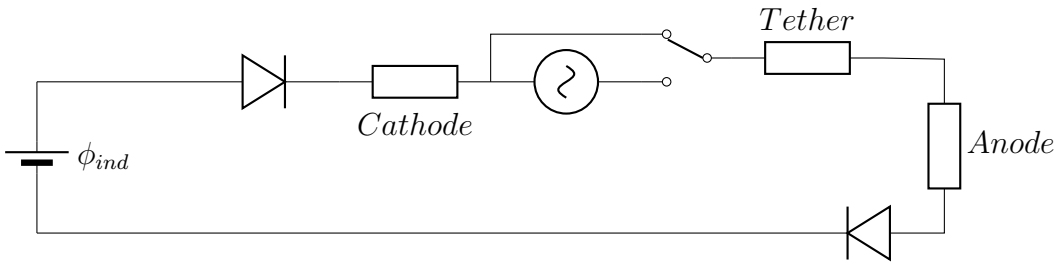

Figure 3: De-orbit/energy harvesting circuit

In the propulsive circuit, the induced electromotive force is reversed, and the generator is substituted with the voltage power supply.

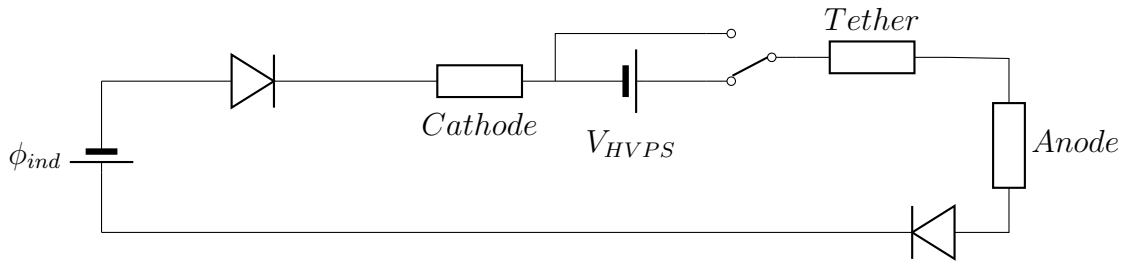

Figure 4: Propulsive circuit

2.2.2 Earth Magnetic field

A crucial variant for the behavior of EDTs is the shape and strength of the magnetic field. Earth's magnetic field can be divided according to its source. The primary and most internal component represents 90% of the total, and it is produced due to the movement of liquid metals in the Earth's core. The external component is generated by solar activity and has an important daily variation [21].

For the purpose of modeling and as simplification, the magnetic field can be represented using only a static version of the internal component. This results in a magnetic dipole of strength $B_0 = 3.15 \cdot 10^{-5}T$, un-tilted and therefore aligned vertically with the axis Z_{GE} (defined in Section 3.1). The mathematical expression of the field is shown in Equation 4.

$$\vec{B} = -B_0 \cdot R_E^3 \cdot \left\{ \frac{3xz}{(x^2+y^2+z^2)^{\frac{5}{2}}}, \frac{3yz}{(x^2+y^2+z^2)^{\frac{5}{2}}}, \frac{(2z^2-y^2-x^2)}{(x^2+y^2+z^2)^{\frac{5}{2}}} \right\} \tag{4}$$

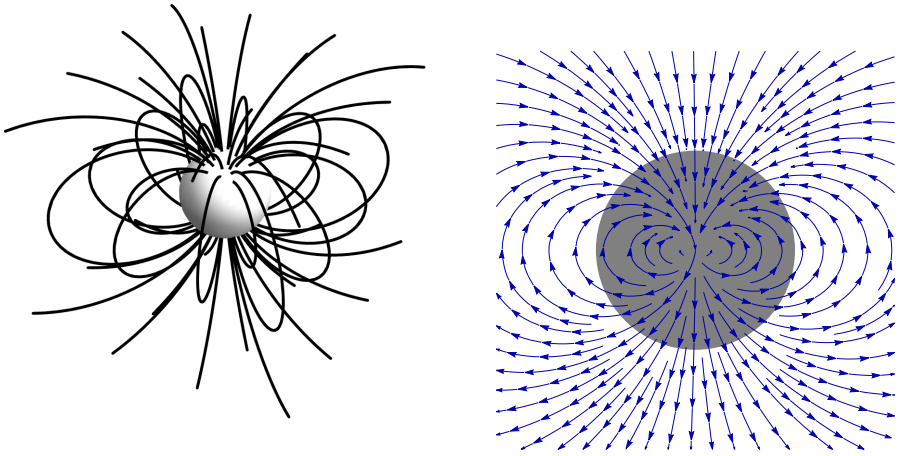

Figure 5: Representation of the Earth's magnetic field as an un-tilted dipole

2.2.3 Ionosphere plasma model

An essential part to close the circuit of the tether is the existence of charged particles in the orbit. As it will be defined in section 2.2.4, the abundance of particles in the ionosphere is a factor in the available current in the anode.

The ionosphere is the upper layer of the atmosphere composed of charged particles ionized by solar radiation. Although the concentration of ions is not constant during the daily cycles, it is possible to average the number of particles, as shown in Figure 6.

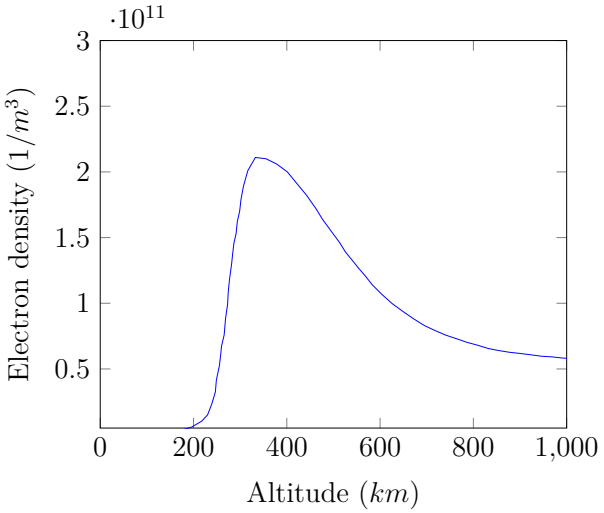

Figure 6: Electron density (n_∞) in LEO orbits as a function of the altitude [2]

2.2.4 Grid sphere electrode current transmission

In order to allow the current to flow into the tether, it is necessary to use a device capable of capturing the electrons present in the ionosphere. A grid sphere contactor (Figure 7) fulfills this requirements.

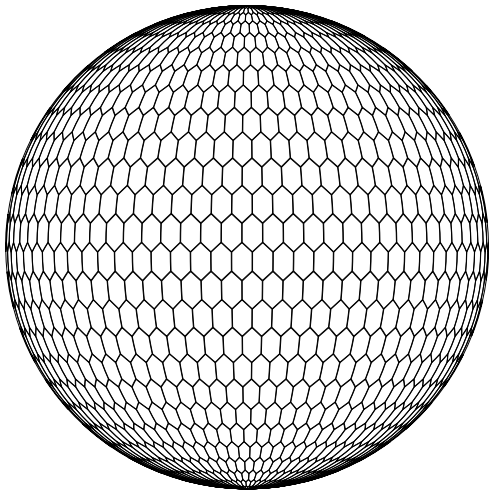

Figure 7: Grid sphere anode schematic representation

The maximum number of electrons (and thus, the maximum current) than can pass through the grid sphere is linked to the electron thermal current in Equation 5 [12]. The current (I_0) is related to the exposed area of the anode (S_{sph}) and to the ambient parameters of electron concentration (n_∞) and electron temperature (T_e). The equation is completed by the Boltzmann's constant (k), the mass of the electron (m_e) and the elementary charge (q_e).

$$I_0 = \frac{1}{4} q_e n_\infty S_{sph} \sqrt{\frac{8kT_e}{\pi m_e}} \tag{5}$$

Then, a correction that relates the electron thermal current and the sphere transparency α (ratio between solid area and total area) is shown in Equation 6.

$$I = 2.372 I_0 (1 - 0.5\alpha^2 - 0.5\alpha^4) \tag{6}$$

3 Equations of movement and perturbations

This section will set the foundations for the simulation of the movement of the satellites. For this purpose, it will be explained the two-body motion problem with perturbations/ external accelerations and the reference frame used for the calculations.

3.1 Reference frames

The choice of a reference frame is conditioned by the problem to be solved. A correct selection, allows to visualize and calculate the solution in a more straightforward and precise manner. To define a reference frame, it is necessary to select: an origin, a plane, and a direction.

In orbital mechanics, the usual reference frames are Heliocentric, Geocentric, Equatorial and Topocentric-Horizon, which are defined according to Table 1.

	Origin	*Plane*	*Direction*
Heliocentric	Sun	Ecliptic plane	First Point of Aries
Geocentric-Equatorial	Earth	Equatorial plane	First Point of Aries
Topocentric-Horizon	Observator	Horizon	South Horizon

Table 1: Reference frame's defining elements

In Section 2.2.2, the magnetic field was defined in a reference frame where $Plane-XY$ was the equator, and $Axis-Z$ was aligned with the rotation axis of the Earth. Taking into consideration that the studied orbits will be only geocentric and the definition of the magnetic field, the most appropriate reference frame is the Geocentric-Equatorial.

3.1.1 Geocentric - Equatorial reference frame

The geocentric reference frame is defined with origin in the center of the Earth, the equator plane as the reference plane, and the First Point of Aries as the reference direction.

The Z-axis is aligned with the Earth's rotating axis, while the X-axis follows the First Point of Aries direction. The Y-axis is oriented to form an orthogonal coordinate system. These axes do not rotate with respect to the stars except for the rotation of the solar system with respect to the center of the galaxy (which is considered negligible). Therefore, the reference frame is inertial.

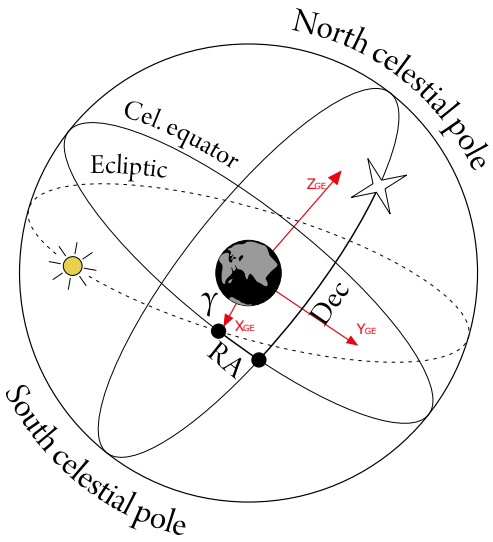

Figure 8: Geocentric - Equatorial reference system[5]

3.2 Two-body equations

Newton's second law says that an object's rate of change of motion is proportional to the sum of all forces applied to it (Equation 7). The change of motion is represented in the first term as the time derivative of the linear momentum ($\vec{p}$), which can be expressed as the product of the mass (m) and the velocity ($\vec{v}$). If the mass is constant, the time derivative is only applied to the velocity vector, which is equal to the acceleration ($\vec{a}$). This result then match the summation of forces.

$$\frac{d\vec{p}}{dt} = \frac{d(m\vec{v})}{dt} = m\vec{a} = \sum \vec{F} \tag{7}$$

Additionally, Newton's law of universal gravitation describes that two bodies attract each other with a force of magnitude of the product of their masses divided by the square of the distance between their centers. The direction of the force would be in the line joining the center of masses and the sense of mutual attraction (Equation 8). To complete the definition, the distance between the bodies is defined as $\vec{r} = \vec{R_2} - \vec{R_1}$, ($\vec{R_1}$ and $\vec{R_2}$ belong to an inertial reference frame, Figure 9).

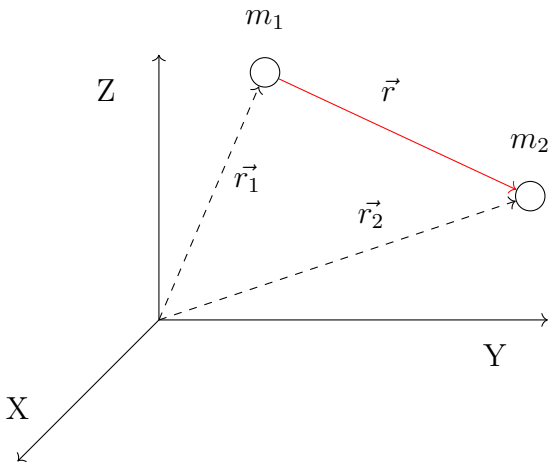

Figure 9: Representation of the bodies in an inertial reference frame

$$\vec{F_{21}} = -\vec{F_{12}} = -G\frac{m_1 m_2}{r^2}\vec{u_r} \tag{8}$$

Therefore, applying Newton's second law to Equation 8, it is possible to express the acceleration to which each body is subjected.

$$\ddot{\vec{R}}_1 = -G\frac{m_2}{r^2}\vec{u_r} \qquad\qquad \ddot{\vec{R}}_2 = G\frac{m_1}{r^2}\vec{u_r} \tag{9}$$

Naming m_2 as M_e and m_1 as m_s, the acceleration between the two bodies $\ddot{\vec{r}}$ is defined in Equation 10. The standard gravitational parameter (μ) is substituted from $G \cdot M_e$ with the assumption that $M_e >> m_s$.

$$\ddot{\vec{r}} = -G\frac{M_e + m_s}{r^2}\vec{u_r} = -\frac{\mu}{r^2}\vec{u_r} \tag{10}$$

This expression in Equation 10 is only valid if the coordinate system used is not rotating ($\vec{\Omega} = \dot{\vec{\Omega}} = 0$), so the absolute acceleration and the relative acceleration are the same (Equation 11).

$$\ddot{\vec{r}} = \ddot{r_{rel}} + \dot{\vec{\Omega}} \times \vec{r_{rel}} + \vec{\Omega} \times (\vec{\Omega} \times \vec{r_{rel}}) + 2(\vec{\Omega} \times \dot{\vec{r_{rel}}}) = \ddot{r_{rel}} \tag{11}$$

3.2.1 Additional forces / Perturbations

The final expression of Equation 10 defines the movement of a body around another, considering only the gravitational effect of a perfectly spherical body. To include other forces such as the drag or the Lorentz force, it is necessary to recall Equation 7. As a result, the original movement is now affected by "perturbations" (Equation 12).

$$m_s\ddot{\vec{r}} = \sum \vec{F} \rightarrow \ddot{\vec{r}} = -\frac{\mu}{r^2}\vec{u_r} + \frac{\vec{F}}{m_s} = -\frac{\mu}{r^2}\vec{u_r} + \sum \vec{p} \tag{12}$$

3.2.2 Drag force as a perturbation

The drag is the force exerted by a fluid, in this case, the atmosphere, on an object due to its relative motion. It is proportional to the density (ρ), the drag coefficient (C_D), a reference surface (S_f) related to the drag coefficient and the square of the relative velocity (v_a).

$$D = \frac{1}{2}\rho S_f C_D v_a^2 \tag{13}$$

Drag coefficient The drag coefficient (C_D) is a dimensionless quantity used to express the dependence of shape, roughness, inclination, and other parameters on the drag force.

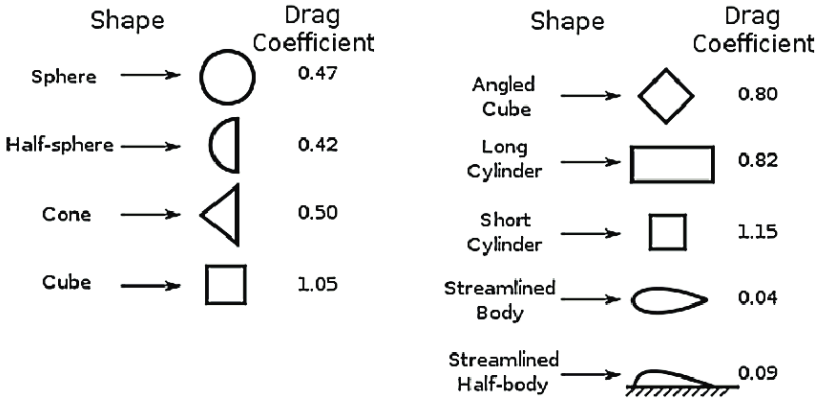

Figure 10: Drag coefficient according to the shape [22]

Aerodynamic velocity The Drag force is proportional to the square of the velocity **relative to the fluid**. Hence, the local velocity of the atmosphere must be subtracted from the one of the satellite. The aerodynamic velocity is then calculated in Equation 14.

$$\vec{v_a} = \vec{v} - \vec{v_{atm}} = \vec{v} - \vec{\omega_E} \times \vec{r} \tag{14}$$

The NRLMSIS 2.0 density model Density is a crucial parameter for drag force in satellites. Beyond the 1000 km of altitude, the influence of the atmosphere is insignificant. Satellites below the 500 km usually need to have propulsion to compensate for the loss of altitude during their mission.

The atmosphere's density in space is dependent on external factors such as solar radiation and geomagnetic activity along the time. For this reason, the model NRLMSIS 2.0 [8] was developed integrating the influence of the most relevant atomic species and their dependence on time (among other interactions). Although NRLMSIS 2.0 provides an excellent model of the atmosphere with time, a static image of the atmosphere of the date 0:00 UTC 1/1/2020 (Figure 11) was integrated in the MATLAB function used to produce the results.

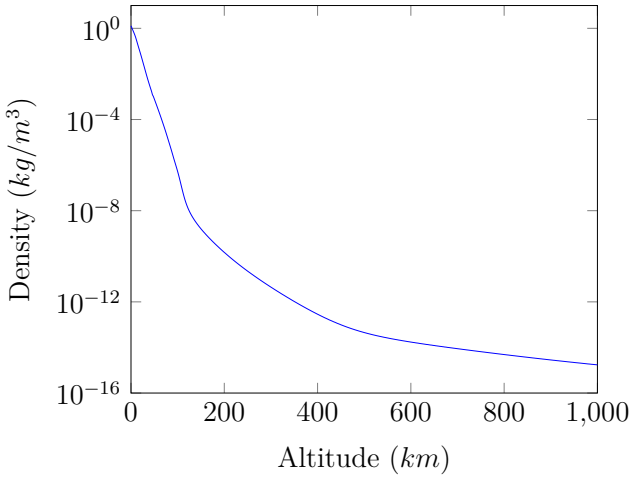

Figure 11: Atmospheric density as a function of altitude

Final perturbation vector Following the expression of Equation 12 and a vectored definition of the drag force of Equation 13 (direction of the velocity vector and opposite sense), the perturbation vector is obtained.

$$\boxed{\vec{p}_{Drag} = \frac{\vec{D}}{m_s} = -\frac{\rho S_f C_D v_a \vec{v_a}}{2m_{sat}}} \tag{15}$$

3.2.3 Lorentz force as a perturbation

Following the same approach as with the drag force, the Lorentz force (2) can be transformed into a perturbation vector dividing it by the mass of the satellite. The final expression is calculated in Equation 16.

$$\frac{\vec{F}_B}{m_{sat}} = \boxed{\vec{p}_B = \pm\left\{-\frac{B_0 I L_0 R_E^3 y}{m_s r^4}, \frac{B_0 I L_0 R_E^3 x}{m_s r^4}, 0\right\}} \tag{16}$$

3.3 Keplerian Orbits

The equation 10 (without the perturbations) describes a Keplerian Orbit's movement, namely, a trajectory that follows a circle, ellipse, parabola, or hyperbola in a 2D plane. The following parameters characterize Kepler orbits:

Angular momentum Represents the quantity of rotational movement. The vector direction is perpendicular to the orbital plane.

$$\vec{h} = \vec{r} \times \vec{v} \tag{17}$$

Laplace-Runge-Lenz vector Describe the shape and orientation of the orbit. It is contained in the orbital plane, and its direction is the same as the semiaxis.

$$\vec{C} = \vec{v} \times \vec{h} - \mu \frac{\vec{r}}{r} \tag{18}$$

Eccentricity vector It is a parameter that determines how the orbit is in relation to a circular one. The value of $(e = 0)$ correspond to a circle, $(0 < e < 1)$ to a ellipse, $(e = 1)$ to a parabola and $(e > 1)$ to an hyperbola. In this study, only circular and elliptic orbits are considered as they are the only ones that do not escape the orbiting body.

$$\vec{e} = \frac{\vec{C}}{\mu} \tag{19}$$

In addition to the constants, it is possible to obtain a relation between the modulus of the orbital radius and the true anomaly (θ).

$$r = \frac{h^2/\mu}{1 + ecos(\theta)} \tag{20}$$

3.3.1 Orbital elements

In order to identify a Kepler orbit unequivocally, there exist a set of parameters known as the orbital elements that situate the orbit from the chosen reference system (Figure 12).

1. Semimajor axis (a): addition of the periapsis and apoapsis distances.
2. Excentricity (e): (as explained) describe the shape of the orbit compared to a circle.
3. Inclination (i): angle between the reference plane and the orbiting plane measured at the ascending node.
4. Longitude of the ascending node (Ω): angle between the reference direction and the ascending node.
5. Argument of the periapsis (ω): orientates the ellipse in the orbiting plane (angle between the ascending node and the periapsis vector).
6. True anomaly (θ): angle between the periapsis and the orbiting body.

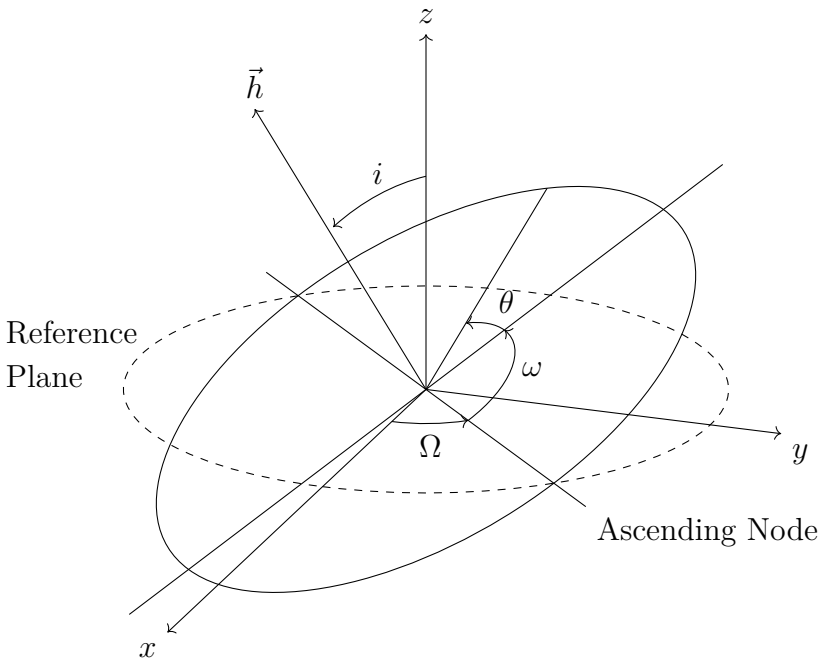

Figure 12: Oribtal elements

4 Applications: Satellite de-orbit

As set out in the previous sections, one of the main applications of electrodynamic tethers is the satellite de-orbit. However, the system's viability depends on the satellite's building parameters and the programmed mission (orbit location and extension).

For this purpose, calculations are performed in 3 groups using MATLAB. The first one of equatorial circular orbits, which represents the most optimal conditions for the tether as the magnetic field is perpendicular to the system and constant along the orbit. The second group determines the efficiency of the system in inclined circular orbits, where the direction of the magnetic field reduces the magnitude of the force. The third and final group measures the variations due to a non-constant magnetic field in elliptic equatorial orbits. To carry on the simulations, the system parameters in Table 2 are maintained constant.

Parameter	*Value*
Tether linear resistance	*2.8e-8* Ω/m
Tether radius (conductive)	*0.5e-3* m
Grid sphere radius	*2* m
Drag coefficient	*0.8* $(-)$

Table 2: System common parameters

In addition to the tether parameters, it is necessary to establish some reference magnitudes consistent with a real satellite. Due to its similarity in mission to the proposed topic, a satellite of the Starlink constellation is used. It is interesting to mention the difference in inclination between the real and fictional satellites. Usually, LEO satellites are not positioned in equatorial orbits because the covered area by inclined orbit satellites has a greater interest that covered by equatorial satellites.

Figure 13: Starlink L1-1 satellite[15]

Parameter	*Starlink L1-1*	*Fictional satellite (base)*
Mass	*260 kg*	*100 kg*
S_f	*6 m^2*	*2 m^2*
h_0	*530 km*	*400 km*
i	53^o	0^o

Table 3: System common parameters [15]

4.1 Equatorial circular orbits

In addition to the common parameters, the type of orbit is defined by the initial conditions of the integrator. To represent a circular orbit ($e = 0$), it is necessary to solve the relation of the orbital parameters defined in Section 3.3.

$$\begin{cases} \vec{h} = \vec{r} \times \vec{v} \rightarrow h = r \cdot v \\ r = \frac{h^2/\mu}{1+ecos(\theta)} = h^2/\mu \end{cases} \rightarrow v = \sqrt{\mu/r} \tag{21}$$

Therefore, the initial conditions for this section are shown in Table 4.

$\vec{r_0}$	$\{r_0, 0, 0\}$
$\vec{v_0}$	$\{0, \sqrt{\mu/r_0}, 0\}$

Table 4: Equatorial circular orbits' initial conditions

Once the initial conditions have been defined, the following parametric tests are defined: mass dependence, altitude dependence, and tether length dependence.

4.1.1 Mass dependence

In movements characterized only by the gravitational force, the satellite mass is independent of the movement (Equation 10) as long as $m_s << M$. However, in the external forces, the satellite's mass acts as a damper, as it reduces the acceleration produced by a force of the same magnitude (Equation 12).

Parameter	*Value*
Satellite mass	*100-1000 kg*
Initial altitude	*400 km*
Tether length	*1 km*

Table 5: System parameters for mass dependence test

The dampening effect of the mass is noticeable in the evolution of the orbital radius (Figure 14). This graph shows that the drag force produces smoother transitions (between h = 150 km and h = 200 km) in heavier satellites than in lighter satellites (considering

the same reference surface and drag coefficient). The same occurs with the Lorentz force's range of action (h > 200-250 km).

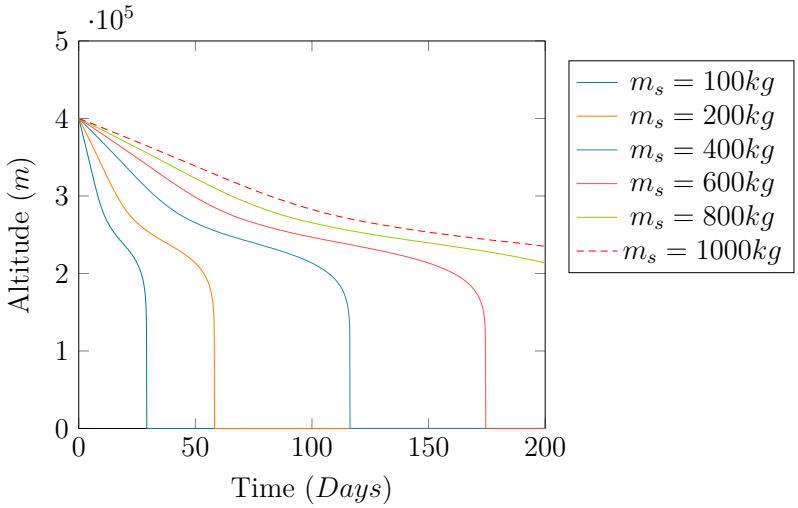

Figure 14: Satellite orbital radius as a function of time and tether mass

Concerning the total de-orbit time: from the activation of the tether to the ground crash, the mass-day relation is linear (Figure 15). This linear relation is caused by the presence of the mass as a divisor in the external forces, which converts to a linear factor when the time is evaluated (Equation 22).

$$a = \frac{dv}{dt} \approx \frac{\Delta v}{\Delta t} = \frac{F}{m_s} \rightarrow \Delta t = \frac{m_s \Delta v}{F} \tag{22}$$

Nevertheless, the de-orbit time is not usually presented only as a function of the mass but as a function of the area/mass ratio due to the intervention of the drag force. In this kind of graph, the relation with the parameter is hyperbolic as the Area remains in the denominator according to Equation 22.

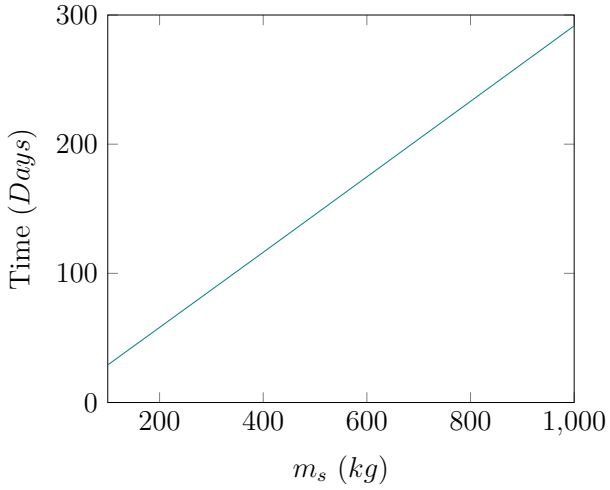

Figure 15: Satellite de-orbit time as a function of the satellite mass

4.1.2 Initial altitude dependence

The initial altitude affect the deorbit trajectory in three different ways. The first one and the most evident, a higher orbital radius takes more time to deorbit than a lower radius. The second reason is the distribution of ions in the ionosphere. The third and final reason is laying inside the atmospheric drag region, where the satellite decay even without the need of other deorbit system. For this reason, the range of the studied radius varies from the atmospheric drag upper boundary (h = 400 km) to the ionosphere upper boundary (h = 800 km) as shown in Table 6.

Parameter	*Value*
Satellite mass	*100 kg*
Initial altitude	*300-1000 km*
Tether length	*1 km*

Table 6: System parameters for altitude dependence test

The distribution of the satellite radius evolution (Figure 16) indicates that the difference in time between h=300 km and h=500km (Δt=18 days) is similar to the difference between h=400 km and h=600 km (Δt=23 days). The similarity relates to the distribution of the electron density (Figure 6). The time difference between h=600 km and h=800 km is more than double than the previous one due to the drop in electron density (Δt=67 days).

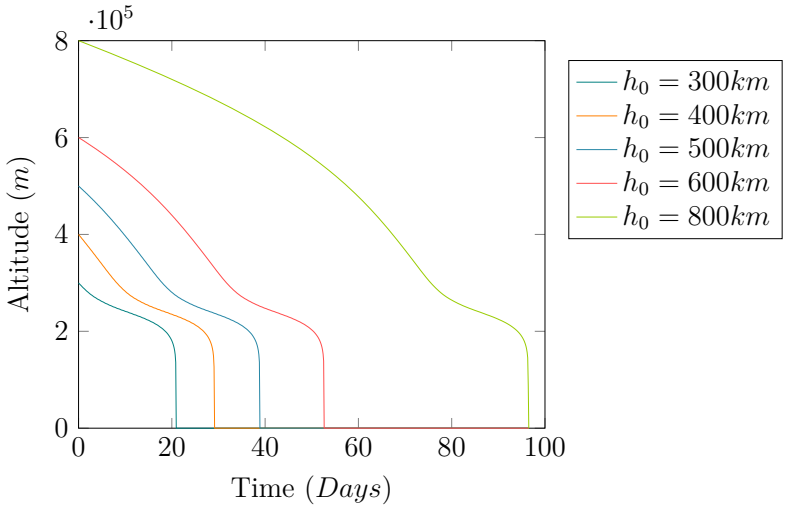

Figure 16: Satellite orbital radius as a function of time and initial altitude

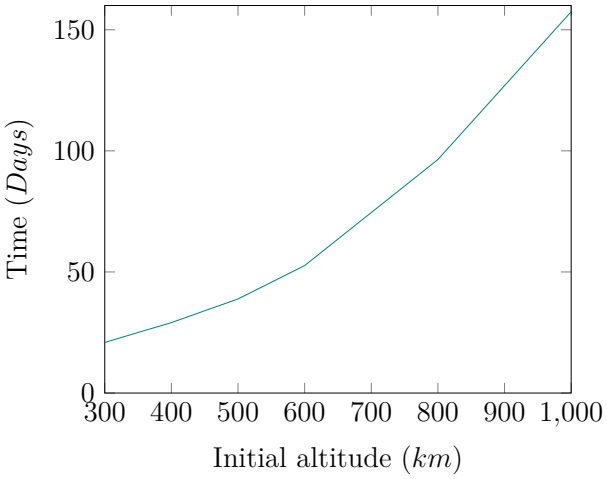

Figure 17: Satellite de-orbit time as a function of the initial altitude

4.1.3 Tether length dependence

The last parameter related to the satellite construction is the length of the tether. The effect of the length is directly shown in the Lorentz Force as a direct factor in the magnitude. However a longer tether also increase the probability of impact with space debris and thus a failure of the system. For this reason, it is necessary to pursue a balance between a reasonable de-orbit time and the probability of failure due to an impact (studied lengths shown in Table 7).

Parameter	*Value*
Satellite mass	*100 kg*
Initial altitude	*400 km*
Tether length	*0.5-10 km*

Table 7: System parameters for tether length dependence test

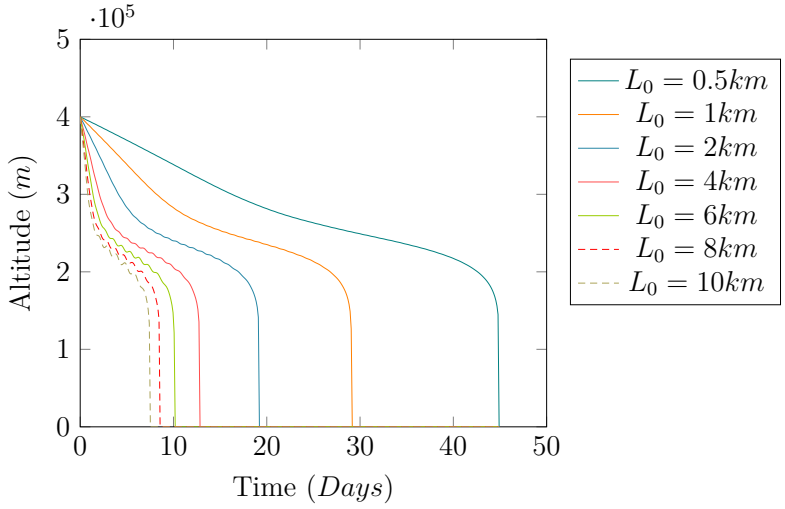

Figure 18: Satellite orbital radius as a function of time and tether length

The distribution of the de-orbit time with respect to the tether length is related to the study of the mass and in particular to the relation obtained in Equation 22. In this case the length is a factor in the force. Being the force in the denominator, the relation between time and tether length is hyperbolic.

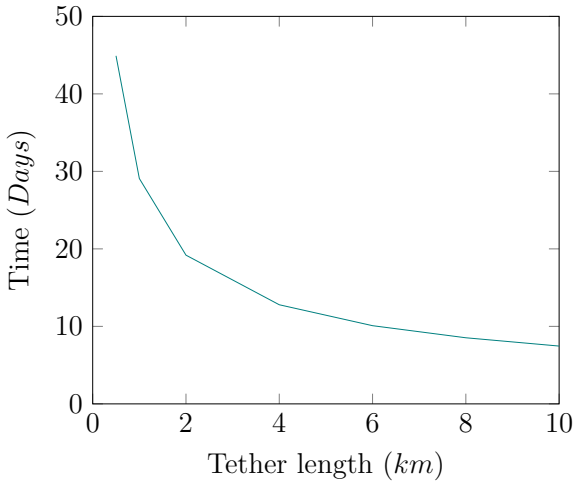

Figure 19: Satellite de-orbit time as a function of the length

4.2 The efficiency with orbit inclination

In order to introduce the inclination as a parameter it is necessary to develop a new expression for the initial conditions. From the relation of the angular momentum and the vector $\{0, 0, 1\}$ is it possible to obtain the orbit inclination. Knowing that in the initial point the orbital radius lays only in the $\{1, 0, 0\}$ direction and with the previous result it is possible to solve v_y and v_z.

$$\begin{aligned} \vec{h} &= \{r_0, 0, 0\} \times \{v_x, v_y, v_z\} = \{0, -r_0 v_z, r_0 v_y\} \\ h &= r_0 \sqrt{v_z^2 + v_y^2} = r_0 \cdot v = r_0 \sqrt{\mu / r_0} = \sqrt{\mu \cdot r_0} \end{aligned} \tag{23}$$

$$\begin{aligned} cos(i) = \frac{(\vec{h} \cdot (0,0,1))}{h} = \frac{r_0 v_y}{\sqrt{\mu \cdot r_0}} \rightarrow \boxed{v_y = cos(i)\sqrt{\frac{\mu}{r_0}}} \\ \sqrt{\mu / r_0} = \sqrt{cos(i)^2 \frac{\mu}{r_0} + v_z^2} \rightarrow \boxed{v_z = sin(i)\sqrt{\frac{\mu}{r_0}}} \end{aligned} \tag{24}$$

$\vec{r_0}$	$\{r_0, 0, 0\}$
$\vec{v_0}$	$\{0, cos(i)\sqrt{\frac{\mu}{r_0}}, sin(i)\sqrt{\frac{\mu}{r_0}}\}$

Table 8: Inclined circular orbits initial conditions

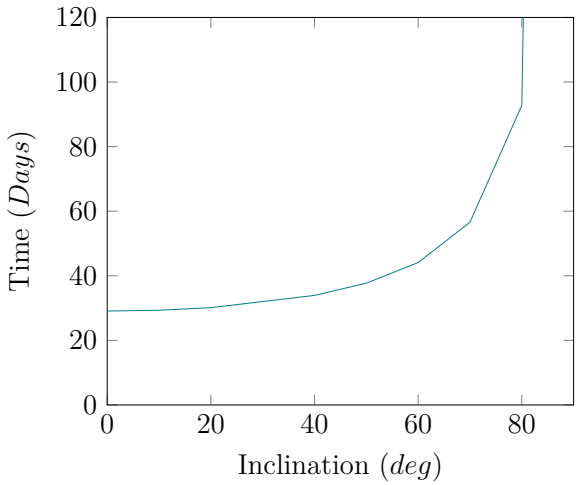

Figure 20: Satellite de-orbit time as a function of the inclination

To justify the behaviour in Figure 20 it is necessary to develop the expression in the direction that produces a greater acceleration or deceleration. A projection in the velocity direction (Equation 25) shows that the effective force is proportional to the cosine of the inclination. Hence, the difference in time is proportional to the inverse of this force, the secant which resemble the figure.

$$\begin{cases} \hat{F_B} = \{-cos(i)sin(\theta), cos(\theta), 0\} \\ \hat{v} = \{-sin(\theta), cos(i)cos(\theta), sin(i)cos(\theta), 0\} \end{cases} \qquad F_{eff} \propto \hat{F_B}.\hat{v} = cos(i) \rightarrow \Delta t \propto \frac{1}{cos(i)} \tag{25}$$

4.3 Efficiency in elliptic orbits

In Section 4.1.2, it was seen that the efficiency of the system decay with the satellite altitude. In elliptic orbits, the radius varies with the true anomaly. For this purpose there will be analyzed eccentricities whose complete orbit lays into the ionosphere effective volume. The eccentricities that fulfil this conditions range between 0 and 0.1. Firstly, it is necessary to introduce the eccentricity in the initial conditions with a similar procedure as the one done in Section 4.2. The known initial point will be fixed as the perigee and together with the expression of Equation 20, the initial conditions are obtained (Table 9).

$$\begin{cases} \vec{h} = \vec{r} \times \vec{v} \rightarrow perigee \rightarrow h = r \cdot v \\ r = \frac{h^2/\mu}{1+ecos(\theta)} \rightarrow \theta = 0 \rightarrow \frac{h^2/\mu}{1+e} \end{cases} \qquad \rightarrow v = \sqrt{\mu(1+e)/r} \tag{26}$$

$\vec{r_0}$	$\{r_0, 0, 0\}$
$\vec{v_0}$	$\{0, \sqrt{\mu(1+e)/r_0}, 0\}$

Table 9: Equatorial elliptic orbits initial conditions

In relation with the tendency shown in Figure 21, it is remarkable to say that eccentricities that do not variate the maximum radius considerably ($< 1\%$) do not affect in a significant way the effectiveness and the de-orbit time. However, with $e = 0.1$ ($h_{max} > 1000km$) the total de-orbit time reaches times similar to the circular orbits of the same semimajor axis a.

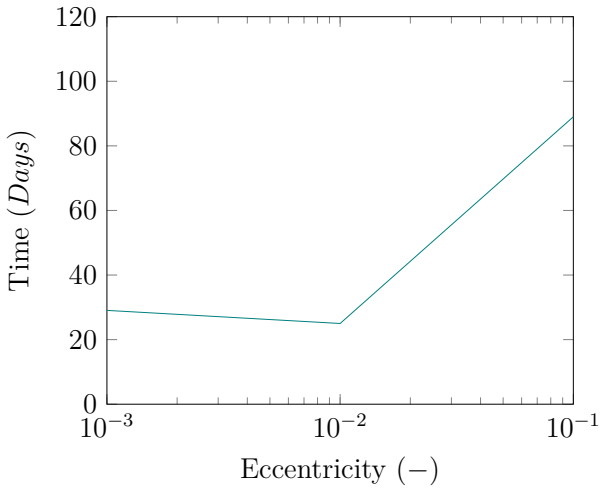

Figure 21: Satellite de-orbit time as a function of the eccentricity

5 Applications: Satellite drag compensation

Following with the second application, it will be described and calculated the viability of an electrodynamic tether system to compensate the drag force (preventing orbital decay) and extend the life of a satellite in VLEO (Very Low Earth Orbits).

5.1 Orbital radius and velocity as a function of the orbital elements

In order to simplify the problem and taking into consideration that the objective is to mitigate the perturbations that depend on time derivatives, the first approach will only consider θ as the independent variable and not its dependence on time. Following with this constrain, the first step is to define the radius and velocity as a function of the orbital elements. The radius can be defined in the orbital plane in the perifocal coordinate system (distance: r, angle:θ). From the orbital plane, three rotations are needed to change to the Geocentric-Equatorial system: longitude of the ascending node, inclination and argument of the periapsis (Shown in figure: 12). As studied orbit will be circular and the studied forces have axial symmetry, the elements ω and Ω are equal to 0 for further simplification. This process is shown in equations 27 and 28.

$$\vec{r} = R_z(-\Omega)R_x(-i)R_z(-\omega)\begin{Bmatrix} r \cdot cos(\theta) \\ r \cdot sin(\theta) \\ 0 \end{Bmatrix} = \begin{Bmatrix} r \cdot cos(\theta) \\ r \cdot cos(i)sin(\theta) \\ r \cdot sin(i)sin(\theta) \end{Bmatrix} \tag{27}$$

$$\vec{v} = R_z(-\Omega)R_x(-i)R_z(-\omega)\begin{Bmatrix} \frac{-\mu}{h}sin(\theta) \\ \frac{\mu}{h}(e + cos(\theta)) \\ \frac{\mu}{h}(e + cos(\theta)) \end{Bmatrix} = \begin{Bmatrix} -\sqrt{\frac{\mu}{r_0}}sin(\theta) \\ \sqrt{\frac{\mu}{r_0}}cos(i)cos(\theta) \\ \sqrt{\frac{\mu}{r_0}}sin(i)cos(\theta) \end{Bmatrix} \tag{28}$$

5.2 Drag compensation theoretical approach

For the purpose of compensating the drag vector and because the vectors are not aligned, it is necessary to define a direction to project the vectors. The direction chosen is the one of the velocity vector, which is also the Drag force direction. Figure 22 shows the projection of the force vectors.

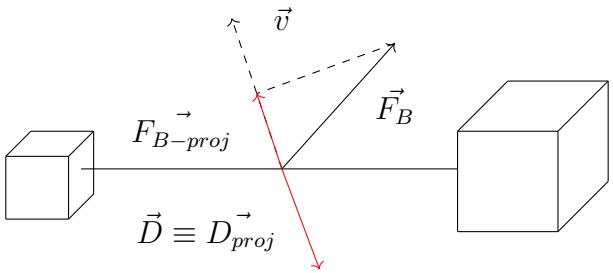

Figure 22: Magnetic and drag vector projection in the velocity vector

In the Drag projection is it possible to consider that the satellite velocity is much greater that the earths rotation speed at the selected orbital radius. Thus, is it possible to simplify the expression with $v \approx v_a$ (Equation 29).

$$D_{proj} = \frac{\vec{D} \cdot v}{|\vec{v}|} = -|\vec{D}| = -\frac{\rho S_f C_D v_a^2}{2} \tag{29}$$

In the Lorentz force projection, the expression is simplified showing that it does not depend on the true anomaly (θ) but only in the cosine of the orbit inclination (Equation 30). This result is similar to the one found in Section 4.2.

$$F_{B-proj} = \frac{\vec{F_B} \cdot v}{|\vec{v}|} = \frac{B_0 I_0 L_0 R_E^3 cos(i)}{r^3} \tag{30}$$

5.3 System limitations

With the projections of the forces, is it possible to isolate the value of the current (Equation 31). This current represents the minimum current that the system needs to counter the drag force.

$$D_{proj} + F_{B-proj} = 0 \rightarrow I_{req} = \frac{\rho S_f C_D v_a^2 r^3}{2 B_0 L_0 R_E^3 cos(i)} \tag{31}$$

In Figure 23, several combinations of orbital altitude and inclination have been tested and expressed as the percentage of the maximum available current defined in Section 2.2.4. The results show that the system is not feasible for altitudes under 240 km and that satellites with altitude of 260 km expose the system to its limits.

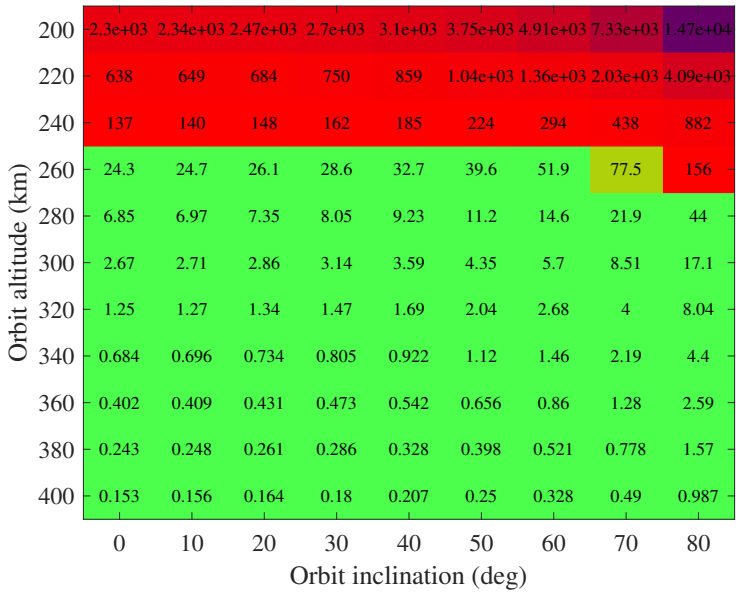

Figure 23: Percentage of the required current out of the maximum available current

6 Validation of results

In order to verify the equations and the results produced, the de-orbiting times from Figure 15 and Figure 20 will be compared to the ones in *Electromagnetic Tethers as Deorbit Devices - Numerical Simulation of Upper-Stage Deorbit Efficiency* [11].

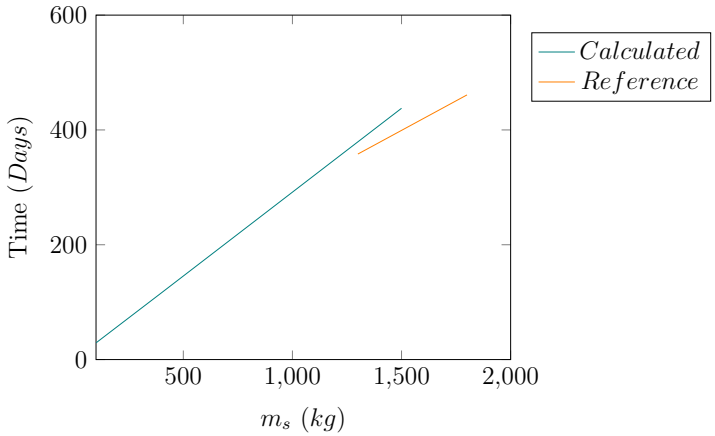

Figure 24: Satellite de-orbit time as a function of the satellite mass (verification)

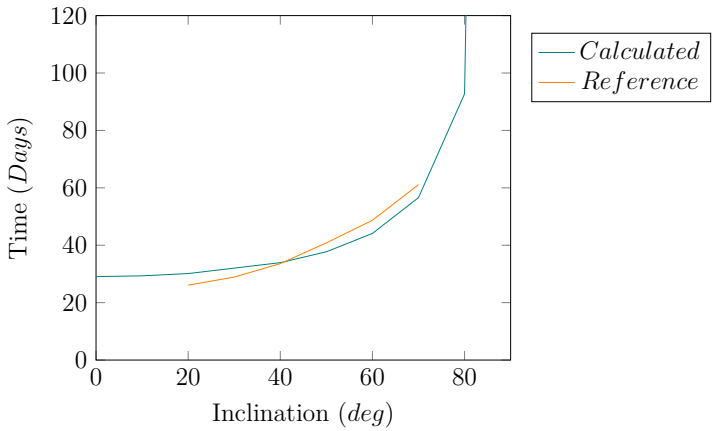

Figure 25: Satellite de-orbit time as a function of the inclination (verification)

Figures 24 and 25 shows that the hypothesis, equations and the implementation used in this academic project produces results that maintain the tendency and magnitude of the results produced in the alternative paper [11], demonstrating the validity of the study.

7 Conclusions

To conclude this bachelor thesis and once all the results has been stated and analysed, it is important to emphasise that the most relevant result of this thesis is the theoretical viability of an electrodynamic tether as a propulsive device. In relation to the rest of the objectives established at the beginning of the present document and with the addition of the obtained results, it is possible to yield the following conclusions:

- Electrodynamic tethers are complex systems that rely on most its components on external factors such as the ion concentration or the strength and direction of the magnetic field.
- The Earth's magnetic field changes with time and cannot be accurately modeled by an algebraic expression. However, significant approximations can be developed for applications in the Low Earth Orbits. The validity of this models lies on the precision needed for the purposed experiments.
- Algebraic models predict in a very accurate way the density of the atmosphere in the lowest layers of it. However empirical models developed in the recent years like the used NRLMSIS 2.0, extend its accuracy up to the limits of the atmosphere allowing to be used in spatial applications.
- Two body equation provides with an accessible method of computing the movement of satellites, allowing to integrate the required drag and Lorenz forces in a simple manner. Moreover, its real benefit lies in the convenience when they are translated into a numerical integrator.
- Electromagnetic tethers in their application as de-orbit devices are limited by some of the orbital elements and the physical characteristics of the system. In the development of an operation with EDTs, the parameters m_s,L_0,i,h_0 and e have to be balanced to produce a reasonable de-orbit time as well as being reliable to failures due to impacts.
- When EDTs are used to mitigate the effect of the drag force, the same parameters used in the de-orbit application have to be recalculated in accordance to the magnitude of the drag force instead of the de-orbit time. Moreover, it is necessary to calculate the necessary voltage that need to be provided by the HVPS to overcome the induced emf. Finally, the non-projected part of the magnetic vector has to be accounted as it may have an effect on the trajectory of the satellite.

Part II
Scope statement

1 Working conditions

1.1 Working space

1. Lighting: regulated by *Real Decreto 486/1997*, workplaces with computers are classified as "moderate-high visual requirements" with a minimum of 200-500 lux.

2. Room temperature: according to *Real Decreto 486/1997*, the temperature in sedentary jobs must lay between 17ºC and 25ºC.

3. Desk table: the space in the desk must guarantee sufficient space to allocate the laptop, peripherals and other necessary material. The distance between the eyes and the laptop display must be around 50 cm.

4. Desk chair: has to be chosen in accordance to the "Ergonomic guide to chose a desk chair"[24] elaborated by the INSST.

1.2 Working materials

Hardware .

- Laptop MSI GS75 8SF:
  - Processor: Intel i7-8750H 4.1GHz
  - RAM: 1x16GB DDR4 2667 MHz
  - Drive: Corsair NVME SSD 1TB
  - Graphics card: Nvidia RTX 2070 16GB
  - Display: 1980x1280 144Hz LED display
  - Operating system: Windows 10 Pro
- External keyboard: Matrics Predator Cherry MX Blue

Internet connection

- Wired Symetrical 600 Mbps connection

Software

- MathWorks®Matlab R2022a: for resolution of numerical differential equations.
- Wolfram Mathematica: for symbolic manipulation of the formulas.
- Overleaf: Online Latex suite.
- Microsoft office 365 Student Edition: Data management with Excel and presentation creation with Powerpoint.
- Tikzit: visual interface for Tikz pictures.

2 Regulatory framework

2.1 Real Decreto 488/1997, de 14 de abril, sobre disposiciones mínimas de seguridad y salud relativas al trabajo con equipos que incluyen pantallas de visualización.[17]

Artículo 1. Objeto .

- El presente Real Decreto establece las disposiciones mínimas de seguridad y de salud para la utilización por los trabajadores de equipos que incluyan pantallas de visualización.
- Las disposiciones de la Ley 31/1995, de 8 de noviembre, de Prevención de Riesgos Laborales, se aplicarán plenamente al conjunto del ámbito contemplado en el apartado anterior.
- Quedan excluidos del ámbito de aplicación de este Real Decreto:

  a) Los puestos de conducción de vehículos o máquinas.

  b) Los sistemas informáticos embarcados en un medio de transporte.

  c) Los sistemas informáticos destinados prioritariamente a ser utilizados por el público.

  d) Los sistemas llamados portátiles, siempre y cuando no se utilicen de modo continuado en un puesto de trabajo.

  e) Las calculadoras, cajas registradoras y todos aquellos equipos que tengan un pequeño dispositivo de visualización de datos o medidas necesario para la utilización directa de dichos equipos.

  f) Las máquinas de escribir de diseño clásico, conocidas como máquinas de ventanilla.

Artículo 2. Definiciones .

A efectos de este Real Decreto se entenderá por:

a) Pantalla de visualización: una pantalla alfanumérica o gráfica, independientemente del método de representación visual utilizado.

b) Puesto de trabajo: el constituido por un equipo con pantalla de visualización provisto, en su caso, de un teclado o dispositivo de adquisición de datos, de un programa para la interconexión persona/máquina, de accesorios ofimáticos y de un asiento y mesa o superficie de trabajo, así como el entorno laboral inmediato.

c) Trabajador: cualquier trabajador que habitualmente y durante una parte relevante de su trabajo normal utilice un equipo con pantalla de visualización.

Artículo 3. Obligaciones generales del empresario .

1) El empresario adoptará las medidas necesarias para que la utilización por los trabajadores de equipos con pantallas de visualización no suponga riesgos para su seguridad o salud o, si ello no fuera posible, para que tales riesgos se reduzcan al mínimo.

   En cualquier caso, los puestos de trabajo a que se refiere el presente Real Decreto deberán cumplir las disposiciones mínimas establecidas en el anexo del mismo.

2) A efectos de lo dispuesto en el primer párrafo del apartado anterior, el empresario deberá evaluar los riesgos para la seguridad y salud de los trabajadores, teniendo en cuenta en particular los posibles riesgos para la vista y los problemas físicos y de carga mental, así como el posible efecto añadido o combinado de los mismos.

   La evaluación se realizará tomando en consideración las características propias del puesto de trabajo y las exigencias de la tarea y entre éstas, especialmente, las siguientes:

   a) El tiempo promedio de utilización diaria del equipo.
   b) El tiempo máximo de atención continua a la pantalla requerido por la tarea habitual.
   c) El grado de atención que exija dicha tarea.

3) Si la evaluación pone de manifiesto que la utilización por los trabajadores de equipos con pantallas de visualización supone o puede suponer un riesgo para su seguridad o salud, el empresario adoptará las medidas técnicas u organizativas necesarias para eliminar o reducir el riesgo al mínimo posible. En particular, deberá reducir la duración máxima del trabajo continuado en pantalla, organizando la actividad diaria

de forma que esta tarea se alterne con otras o estableciendo las pausas necesarias cuando la alternancia de tareas no sea posible o no baste para disminuir el riesgo suficientemente.

4) En los convenios colectivos podrá acordarse la periodicidad, duración y condiciones de organización de los cambios de actividad y pausas a que se refiere el apartado anterior.

Artículo 4. Vigilancia de la salud .

1. El empresario garantizará el derecho de los trabajadores a una vigilancia adecuada de su salud, teniendo en cuenta en particular los riesgos para la vista y los problemas físicos y de carga mental, el posible efecto añadido o combinado de los mismos, y la eventual patología acompañante. Tal vigilancia será realizada por personal sanitario competente y según determinen las autoridades sanitarias en las pautas y protocolos que se elaboren, de conformidad con lo dispuesto en el apartado 3 del artículo 37 del Real Decreto 39/1997, de 17 de enero, por el que se aprueba el Reglamento de los servicios de prevención. Dicha vigilancia deberá ofrecerse a los trabajadores en las siguientes ocasiones:

   a) Antes de comenzar a trabajar con una pantalla de visualización.
   b) Posteriormente, con una periodicidad ajustada al nivel de riesgo a juicio del médico responsable.
   c) Cuando aparezcan trastornos que pudieran deberse a este tipo de trabajo.

2. Cuando los resultados de la vigilancia de la salud a que se refiere el apartado 1 lo hiciese necesario, los trabajadores tendrán derecho a un reconocimiento oftalmológico.

3. El empresario proporcionará gratuitamente a los trabajadores dispositivos correctores especiales para la protección de la vista adecuados al trabajo con el equipo de que se trate, si los resultados de la vigilancia de la salud a que se refieren los apartados anteriores demuestran su necesidad y no pueden utilizarse dispositivos correctores normales.

Artículo 5. Obligaciones en materia de información y formación .

1. De conformidad con los artículos 18 y 19 de la Ley de Prevención de Riesgos Laborales, el empresario deberá garantizar que los trabajadores y los representantes de los trabajadores reciban una formación e información adecuadas sobre los riesgos derivados de la utilización de los equipos que incluyan pantallas de visualización, así como sobre las medidas de prevención y protección que hayan de adoptarse en aplicación del presente Real Decreto.

2. El empresario deberá informar a los trabajadores sobre todos los aspectos relacionados con la seguridad y la salud en su puesto de trabajo y sobre las medidas llevadas a cabo de conformidad con lo dispuesto en los artículos 3 y 4 de este Real Decreto.

3. El empresario deberá garantizar que cada trabajador reciba una formación adecuada sobre las modalidades de uso de los equipos con pantallas de visualización, antes de comenzar este tipo de trabajo y cada vez que la organización del puesto de trabajo se modifique de manera apreciable.

Artículo 6. Consulta y participación de los trabajadores .

La consulta y participación de los trabajadores o sus representantes sobre las cuestiones a que se refiere este Real Decreto se realizarán de conformidad con lo dispuesto en el apartado 2 del artículo 18 de la Ley de Prevención de Riesgos Laborales.

Disposición transitoria única. Plazo de adaptación de los equipos que incluyan pantallas de visualización .

Los equipos que incluyan pantallas de visualización puestos a disposición de los trabajadores en la empresa o centro de trabajo con anterioridad a la fecha de entrada en vigor del presente Real Decreto deberán ajustarse a los requisitos establecidos en el anexo en un plazo de doce meses desde la citada entrada en vigor.

Disposición final primera. Elaboración de la Guía Técnica para la evaluación y prevención de riesgos .

El Instituto Nacional de Seguridad e Higiene en el Trabajo, de acuerdo con lo dispuesto en el apartado 3 del artículo 5 del Real Decreto 39/1997, de 17 de enero, por el que se aprueba el Reglamento de los Servicios de Prevención, elaborará y mantendrá actualizada una Guía Técnica para la evaluación y prevención de los riesgos relativos a la utilización de equipos que incluyan pantallas de visualización.

Disposición final segunda. Habilitación normativa .

Se autoriza al Ministro de Trabajo y Asuntos Sociales para dictar, previo informe de la Comisión Nacional de Seguridad y Salud en el Trabajo, las disposiciones necesarias en desarrollo de este Real Decreto y, específicamente, para proceder a la modificación del anexo del mismo para aquellas adaptaciones de carácter estrictamente técnico en función del progreso técnico, de la evolución de las normativas o especificaciones internacionales o de los conocimientos en el área de los equipos que incluyan pantallas de visualización.

2.2 Contenido mínimo del Trabajo Fin de Grado (TFG) (ETSID)

Como segunda opción se puede realizar el TFG utilizando el siguiente índice de contenidos mínimos:

1. **Memoria**

   Es un documento justificativo y descriptivo de la solución adoptada que incluye el proceso de génesis de la misma, con la indicación de las principales dificultades encontradas y los procesos seguidos en su resolución. También suele hacer referencia a los estudios de viabilidad económica, instrucciones de manejo, planes de ejecución, instalación, puesta en marcha y explotación, aunque estos se desarrollen con más detalle en los anejos a la memoria.

   El índice propuesto es el siguiente:

   1.**1** Objeto

   1.**2** Estudio de necesidades, factores a considerar: limitaciones y condicionantes.

   1.**3** Planteamiento de soluciones alternativas y justificación de la solución adoptada

   1.**4** Descripción detallada de la solución adoptada

   1.**5** Justificación detallada de los elementos o componentes de la solución adoptada (cálculo y dimensionamiento)

   Anexos a la memoria (en función del tipo y necesidades del TFG)

   A.**1** De cálculo (para todas las especialidades, si son muy voluminosos o no aparecen en el apartado 1.5)

   A.**2** Estudio económico.

   A.**3** Manual de usuario.

2. **Planos**

   Los planos constituyen la especificación gráfica del TFG. Este puede contener tanto planos, como esquemas o diagramas, pero no conviene olvidar las características propias de cada tipo de representación ni las Normas ISO a la hora de su utilización. (En caso de no desarrollar este apartado se deberá justificar).

3. **Pliego de condiciones**

   El pliego de condiciones, junto con los planos, constituyen extensiones del contrato entre propiedad y contratista para la ejecución de un TFG, y como tales deben intentar responder, junto al resto de cláusulas del contrato, a las preguntas: ¿qué?, ¿cómo?, ¿cuándo?, ¿cuánto?, y ¿qué ocurre si no se cumple?.

   Con los planos se pretende responder al ¿qué? y ¿cómo? de manera gráfica y con el pliego de condiciones al resto de cuestiones de manera escrita. Obligatoriamente, se consignarán las especificaciones técnicas con los siguientes apartados:

1 Objeto

2 Condiciones de los materiales

- Descripción
- Control de calidad

3 Condiciones de ejecución

- Descripción
- Control de calidad

4 Pruebas y ajustes finales o de servicio

Opcionalmente, en función del alcance del Pliego de Condiciones se incluirán las especificaciones facultativas, legales y económicas.

4. **Presupuesto**

El presupuesto del TFG es el documento que tiene por finalidad dar una idea lo más aproximada posible del importe de su realización.

Podrá realizarse por cualquiera de los métodos establecidos, ya sea por:

- Costes según naturaleza
- Precios descompuestos
- Secciones homogéneas

Part III
Budget

In this part, there will be stated the total costs of this project. There will be included the cost of the computer equipment used, the software licences and the energy consumed by the equipment and the room used in the elaboration of this project. In addition it will be estimated the hourly labor cost of a non-graduated student and its supervisor.

1 Hardware

The cost of the equipment is calculated according its initial cost and the usage time. The maximum annual depreciation rates are stated in *Article 12 of Law 27/2014*.

	Initial cost	Depreciation rate	Usage	Total cost (€)
MSI GS75-8SF 16GB RAM	1899 €	25%	2 months	79.12
Total				**79.12**

Table 10: Hardware costs

2 Software

Software cost is calculated depending on the type of licence model: perpetual or subscription. Perpetual licences are subjected to *Article 12 of Law 27/2014*. However the subscription model is calculated directly as a proportion of the subscription period and the cost per period.

	Licence Type	Cost/period (€)	Usage	Total cost (€)
Matlab 2022a	Yearly	302.50	2 months	50.41
Mathematica Students	Yearly	204.50	2 months	34.08
Office 365 Student	Yearly	0	2 months	0
Overleaf Personal	Monthly	5	2 months	10
Total				**94.49**

Table 11: Software costs

3 Energy

The devices accounted for the energy cost are limited to the ones used in the working place.

	Power (W)	Usage (h)	Energy (kWh)	kWh price	Total cost (€)
Computer	250W	308	77.00	0.326 €	25.10
Lighting	3 x 5W	308	4.62	0.326 €	1.50
Total					**26.60**

Table 12: Energy costs

4 Labor

From the service of human resources of the UPV, the hourly cost is estimated for a Phd and a student with the roll of "assistant".

	Time (h)	Cost per hour (€)	Total (€)
Student	308	10	3080
Supervisor	25	16	400
Total			**3480**

Table 13: Labor costs

5 Total cost

	Total (€)
Hardware	79.12
Software	94.49
Energy	26.60
Labor	3480.00
Total	**3680.21**

Table 14: Total costs

References

[1] The drag coefficient. Available at `https://www.grc.nasa.gov/www/k-12/airplane/dragco.html`.

[2] G. Allegri. Analysis of the effects of simulated synergistic leo environment on solar panels. *54th International Astronautical Congress of the International Astronautical Federation, the International Academy of Astronautics, and the International Institute of Space Law*, 2003.

[3] S. Bilen, J. McTernan, B. Gilchrist, I. Bell, N. Voronka, and R. Hoyt. Electrodynamic tethers for energy harvesting and propulsion on space platforms. *AIAA SPACE 2010 Conference &; Exposition*, 2010.

[4] CNES, Apr 2015. Available at `https://demeter.cnes.fr/en/DEMETER/index.htm`.

[5] W. Commons. Equatorial coordinate system, 2001.

[6] H. D. Curtis. *Orbital Mechanics for Engineering Students*. Elsevier, BH, Butterworth-Heinemann is an imprint of Elsevier, 2019.

[7] R. N. DeWitt, D. Duston, and A. K. Hyder. *The Behavior of Systems in the Space Environment*. European Office of Aerospace Research, 1991.

[8] J. T. Emmert, D. P. Drob, J. M. Picone, D. E. Siskind, M. Jones, M. G. Mlynczak, P. F. Bernath, X. Chu, E. Doornbos, and B. e. a. Funke. Nrlmsis 2.0: A whole-atmosphere empirical model of temperature and neutral species densities. *Earth and Space Science*, 8(3), 2021.

[9] ETSID. Contenido minimo del TFG, 2019.

[10] K. Fuhrhop, E. Choiniere, B. Gilchrist, S. Bilén, and B. West. Current collection to electrodynamic tether systems in space. *2nd International Energy Conversion Engineering Conference*, 2004.

[11] A. Ionel. Electromagnetic Tethers as Deorbit Devices-Numerical Simulation of Upper-Stage Deorbit Efficiency. *International Journal of Advanced Research in Electrical, Electronics and Instrumentation Engineering*, 3297, 2007.

[12] G. Khazanov, E. Krivorutsky, and L. Johnson. Electrodynamic tether as a thruster for leo mission applications. *42nd AIAA/ASME/SAE/ASEE Joint Propulsion Conference & Exhibit*, 2006.

[13] G. V. Khazanov, E. Krivorutsky, and R. B. Sheldon. Solid and grid sphere current collection in view of the tethered satellite system tss 1 and tss 1r mission results. *Journal of Geophysical Research*, 110(A12), 2005.

[14] F. Knorn. M-code latex package, Nov 2015.

[15] G. Krebs. Starlink block v1.0. Available at `https://space.skyrocket.de/doc_sdat/starlink-v1-0.htm`.

[16] J. Lim and J. Chung. Removal of captured space debris using a tethered satellite system. *Journal of Mechanical Science and Technology*, 33(3):1131–1140, 2019.

[17] Ministerio de Trabajo y Asuntos Sociales. Real Decreto 488/1997, de 14 de abril, sobre disposiciones mínimas de seguridad y salud relativas al trabajo con equipos que incluyen pantallas de visualización, 1997.

[18] J. A. Moraño Fernández. Ecuaciones del movimiento en un sistema inercial y en uno relativo. 2019.

[19] J. A. Moraño Fernández. Parámetros constantes en órbitas keplerianas. 2019.

[20] J. A. Moraño Fernández. Órbitas en tres dimensiones: Sistemas de Coordenadas. 2021.

[21] I. G. Nacional. Geomagnetismo. Available at `https://www.ign.es/web/ign/portal/teoria-geomagnetismo`.

[22] NASA. Shape effects on drag.

[23] S. R. Omar, R. Bevilacqua, D. Guglielmo, L. Fineberg, J. Treptow, S. Clark, and Y. Johnson. Spacecraft deorbit point targeting using aerodynamic drag. *Journal of Guidance, Control, and Dynamics*, 40(10):2646–2652, 2017.

[24] M. Peñahora, G. Sanz, and T. Álvarez Bayona. Criterios ergonómicos para la selección de sillas de oficina Ergonomic criteria for the selection of office chairs Critères ergonomiques pour la sélection de chaises de bureau. Technical report, 2018.

Part IV

Annex I: Integrating function

```
1
2  function dr =  gravitatoryLorentz(t,r)
3
4  load datasat.mat
5
6  IO = double(datasat(1));              % Operating mode
7  L0 = double(datasat(2));              % Tether length
8  msat = double(datasat(3));            % Satellite's mass
9  mu = double(datasat(4));              % Gravitational parameter of the ...
       Earth
10 tmax = double(datasat(5));            % Maximmum time of integration
11 CD = double(datasat(6));              % Drag coefficient of the satellite
12 Sfront = double(datasat(7));          % Reference surface of the satellite
13 RE = double(datasat(9));              % Earth's radius
14 ele = double(datasat(10));            % Electron charge
15 Te = double(datasat(11));             % Ion temperature
16 me = double(datasat(12));             % Electron mass
17 k = double(datasat(13));              % Boltzman constant
18 SphSurf = double(datasat(14));        % Surface of the grid sphere
19 RT0 = double(datasat(15));            % Resistance of the tether
20 B0 = double(datasat(16));             % Dipole strength
21
22
23 Oearth = [0,0,(2*pi/(24*3600))];      % Earth angular speed
24
25 waitbar(t/tmax)                       % To update the process waitbar
26
27 x = r(1);
28 xdot = r(2);
29 y = r(3);
30 ydot = r(4);
31 z = r(5);
32 zdot = r(6);
33
34 rmod = sqrt(x^2+y^2+z^2);             % Module of the radius
35 vmod = sqrt(xdot^2+ydot^2+zdot^2);    % Module of the velocity
36
37 %% Radiation model
38
39 h = rmod - RE;                        % Altitude
40
41 ehdata=[0,50,104.8494491,127.66079,150.458926,...% Not shown fully
42 nedata=[2e+4,2e+4,3.39e+05,1.88e+09,1.60e+09,... % Not shown fully
43
```

```
44
45 nefunc = griddedInterpolant(ehdata,nedata,'nearest'); % Plasma ...
       density function
46
47
48 I1 = 0.25*ele*nefunc(h)*SphSurf*sqrt((8*k*Te)/(pi*me)); % Electron ...
       current
49 I0 = 2.372*I1*IO;
50
51
52 %% Lorentz
53
54 FLx = ...
       -(-(863307622649607*I0*L0*y*z^2)/(37437335978537411918220492800000...
55 *(x^2/40589641000000 + y^2/40589641000000 + ...
       z^2/40589641000000)^(5/2)*(x^2 + y^2 + z^2)^(1/2)) - ...
       (287769207549869*I0*L0*y*(x^2/40589641000000 + y^2/40589641000000 ...
       - z^2/20294820500000))/(9223372036854775808*(x^2/40589641000000 +...
56 y^2/40589641000000 + z^2/40589641000000)^(5/2)*(x^2 + y^2 + z^2)^(1/2)));
57 FLy = ...
       -((863307622649607*I0*L0*x*z^2)/(37437335978537411918220492800000...
58 *(x^2/40589641000000 + y^2/40589641000000 + ...
       z^2/40589641000000)^(5/2)*(x^2 + y^2 + z^2)^(1/2)) + ...
       (287769207549869*I0*L0*x*(x^2/40589641000000 + y^2/40589641000000 ...
       - z^2/20294820500000))/(9223372036854775808*(x^2/40589641000000 +...
59 y^2/40589641000000 + z^2/40589641000000)^(5/2)*(x^2 + y^2 + z^2)^(1/2)));
60 FLz = 0;
61
62
63
64 ALx = FLx/msat;
65 ALy = FLy/msat;
66 ALz = FLz/msat;
67
68 %% Gravity
69
70 AGx = -mu*x/rmod^3;
71 AGy = -mu*y/rmod^3;
72 AGz = -mu*z/rmod^3;
73
74
75
76 %% Drag
77
78 hdata = transpose((0:2:1000)*1000);
79 rhodata = [1.291e-03,1.032e-03,8.226e-04,6.590e-04... % Not shown fully
80
81 rhofunc = griddedInterpolant(hdata,rhodata,'nearest');
82
83
84
```

```
85  vvec = [xdot ydot zdot];
86  vaero = vvec - cross(Oearth,[x y z]);  % Aerodynamic velocity
87  vaeromod = norm(vaero);
88  rhoval = rhofunc(h);
89  FDt = -0.5*rhoval*Sfront*CD*vaeromod^2*(vaero/vaeromod);
90
91
92  FDx = FDt(1);
93  FDy = FDt(2);
94  FDz = FDt(3);
95
96
97  ADx = FDx/msat;
98  ADy = FDy/msat;
99  ADz = FDz/msat;
100
101
102
103 %% Total
104
105 xdotdot = AGx + ALx + ADx;
106 ydotdot = AGy + ALy + ADy;
107 zdotdot = AGz + ALz + ADz;
108
109 dr = zeros(size(r));
110
111 dr(1)=xdot;
112 dr(2)=xdotdot;
113 dr(3)=ydot;
114 dr(4)=ydotdot;
115 dr(5)=zdot;
116 dr(6)=zdotdot;
117
118 end
```